Mobile Bluetooth Mesh Networks: Performance Evaluation of a Novel Concept

Zohreh Hosseinkhani, Carles Gomez, Majid Nabi, *Member, IEEE*

***Abstract*— The Bluetooth SIG released Bluetooth Mesh (BM) as a potential networking technology for Internet of Things (IoT) networks. The use of BM technology in various applications has become increasingly popular. However, most BM studies in the literature assume networks comprising only static nodes or a low number of mobile devices. In this paper, we introduce and explore the novel concept of Mobile Bluetooth Mesh Networks (MBMNs), which are composed of BM-enabled mobile devices, such as smartphones carried by people. MBMNs can be created opportunistically in a wide range of environments and for various purposes. We argue that MBMNs can be a proper networking solution for many applications, thanks to the native support of topology dynamics by the flooding-based end-to-end data delivery of the protocol. This paper presents and evaluates the performance of MBMNs and explores the impact of various conditions and parameters on these networks. Additionally, we conduct real-world experiments to demonstrate that MBMNs are feasible and offer relatively good performance.**

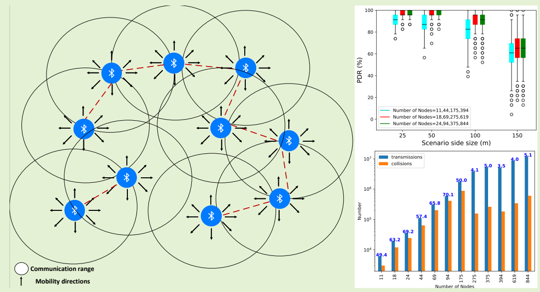

***Index Terms*— Bluetooth Mesh, Mobile network, Performance study, Mobile Bluetooth Mesh Network.**

I. INTRODUCTION

BLUETOOTH Low Energy (BLE) is a low-power, short-range wireless technology that has become a fundamental Internet of Things (IoT) enabler. As of the writing, annual shipments of BLE-enabled devices are estimated as 4 billion, with an expectation to further increase in the next few years (e.g., up to 6 billion by 2025) [1]. BLE is a prominent low-power technology in the consumer electronics market, as it is present in most smartphones, it is also dominant in tablets and wearables, and it is used in many IoT applications [2] [3].

The original BLE design was based on a simple star topology network, intended to enable the communication between resource-constrained devices (e.g., sensors) and a central, more powerful device (e.g., a smartphone). However, the coverage and robustness limitations of BLE star topology networks triggered a range of initiatives in order to enable BLE mesh networks [4]. A milestone in this field was achieved in 2017, with the publication of the Bluetooth Mesh (BM) specifications by the Bluetooth Special Interest Group (SIG), which provide a standard approach to enable BLE mesh networks [5]. BM is increasingly being deployed, with current studies forecasting that BM annual shipments will surpass 1 billion by 2026 [1].

The widespread availability of BLE-enabled devices, along with the increasing popularity of BM, provides a basis that can be exploited to create novel applications of BM networks [6]. In this paper, we present and evaluate the performance of Mobile Bluetooth Mesh Networks (MBMNs). An MBMN is composed of BM-enabled mobile devices, such as smartphones carried by humans. The MBMN may be created opportunistically, in a wide variety of environments (e.g., in streets, homes, offices, shopping centers, factories, hospitals, etc.) as long as there is a sufficient device density. The MBMN may be used for many purposes, such as social communication, crowdsensing, IoT data collection or backup communication means (e.g. when Wi-Fi or cellular infrastructure is not available). Two decades ago, the formation of classic Bluetooth multi-hop networks (called scatternets) attracted the attention of the research community [7] [8]. However, the concept did not succeed in practice, in part due to the complexity of the related mechanisms (in contrast, BM is based on a simple, connectionless flooding paradigm for end-to-end data delivery), and also because the penetration levels of classic Bluetooth-enabled mobile phones were not as high as today's omnipresence of BLE-enabled smartphones.

In the literature, most BM studies assume BM networks comprising only static nodes [9] [10] [11], or including a low number of mobile devices within a majority of static nodes [12]–[15]. This is due to the original focus on typical IoT use cases, where most devices are usually static, and also because BM devices in charge of message relaying need to be always on, thus they are typically assumed to be powered by means of the electricity grid. As a result, MBMNs remain currently unexplored. We claim that MBMNs are feasible, considering that the flooding-based end-to-end data delivery

Zohreh Hosseinkhani is with the Department of Electrical and Computer Engineering, Isfahan University of Technology, Isfahan, Iran (email: z.hosseinkhani@ec.iut.ac.ir). Carles Gomez is with the Dept. of Network Engineering, Universitat Politecnica de Catalunya (e-mail: carles.gomez@upc.edu). Majid Nabi (corresponding author) is with the Department of Electrical Engineering, Eindhoven University of Technology, Eindhoven, the Netherlands (email: m.nabi@tue.nl).

This article has been accepted for publication in IEEE Sensors Journal. This is the author's version which has not been fully edited and content may change prior to final publication. Citation information: DOI 10.1109/JSEN.2025.3545249

of BM is suitable for dynamic topologies, and the fact that an MBMN device, such as a smartphone, may stay always on within the lifetime of its battery (which is frequently recharged anyway). Furthermore, we find that the results from extensive simulations and real-world implementations demonstrate that MBMNs exhibit acceptable performance. However, similar to static BM networks, MBMNs are also limited by flooding-based transmission, which can lead to saturated relay nodes. To summarize, the key contributions of this paper are as follows.

1) We investigate and show the feasibility and acceptable performance of MBMNs, primarily due to the adaptability of the flooding-based data dissemination of BM in accommodating dynamic topologies. Moreover, the continuous availability of BLE devices, such as smartphones, that can remain continuously powered on throughout the entire lifespan of their batteries enhances the practicality and convenience of MBMNs.
2) Extensive investigations have been conducted to evaluate the performance of MBMNs across different network sizes and conditions. We conduct a comprehensive comparison of static and mobile networks, examining the impact of different node speeds. Our findings reveal that static networks are significantly influenced by their topology, resulting in varied PDR outcomes. In contrast, mobile networks demonstrate more consistent PDR performance across different speeds. The impact of essential configuration parameters of MBMNs, including the ratio of packet generation and advertising intervals, as well as the effect of the number of retransmissions has been thoroughly examined to assess their influence on MBMN's performance.
3) To substantiate the acceptable performance of MBMNs, real experiments were conducted utilizing Nordic Chip nRF52840 dongles. Through these experiments, the performance of MBMNs was analyzed. The obtained results demonstrate an end-to-end Packet Delivery Ratio (PDR) exceeding 90% across various environments and network sizes.

The remainder of this article is organized as follows. Section II presents an overview of the BM technology. In Section III, related work is discussed. Section IV provides an MBMN performance evaluation by means of simulation and analyzes the obtained results. Section V discusses experiments conducted in a real-world environment. Study limitations are discussed in Section VI. Section VII concludes the paper.

II. Bluetooth Mesh overview

The BM protocol stack consists of several layers, each with its own set of responsibilities, namely: the Model layer, the Foundation Model layer, the Access layer, the Upper Transport layer, the Lower Transport layer, the Network layer, and the Bearer layer.

The Model layer defines application models intended for users, such as lighting and sensing. The Foundation Model layer specifies models, states, and messages for configuring and managing the network. The Access layer governs how the upper layers utilize the upper transport layer, including defining the application data format and controlling the application data encryption and decryption. The Upper Transport layer encrypts, decrypts, and authenticates application data and provides confidentiality in access messages. Additionally, it defines control messages to manage this layer. The Lower Transport layer performs segmentation and reassembly for upper transport messages. The Network layer handles addressing transport messages and determines whether a message should be forwarded to other nodes or rejected. The Bearer layer is responsible for transmitting network messages between nodes. There are two types of bearers at this layer: the GATT bearer and the advertising bearer [16]. The former is based on communicating over an established connection between two BLE neighbors. The latter leverages the periodic transmission of advertisements by a BLE device as means to carry messages.

A. Bluetooth Low Energy Core Specification

BLE physical layer comprises 40 channels in the 2.4 GHz frequency band, each with a 2 MHz bandwidth. The 37th, 38th, and 39th channels are advertising channels, while the rest are data channels. Device discovery and connection establishment occur on the advertising channels, after which the sender and receiver use data channels for sending and receiving packets [17]. In addition, advertising channels are used for broadcasting, as in the case of BM networks. The physical layer bit rate in Bluetooth 4.x is 1 Mbps, while in Bluetooth 5, it ranges from 125 kbps to 2 Mbps [18] [19].

B. Packet Transmission in BM Networks

Advertising and scanning procedures are used for sending and receiving data packets in the BM protocol. The non-connectable and non-scannable undirected advertising events of BLE, without any connection establishment between receivers and senders, are used in the BM packet transmissions. In an advertising event, data packets are sent in the three advertising channels in turn. The *advertising interval* (T_{adv}) is the time between two consecutive advertising events, which is an integer multiple of $0.625\ ms$ in the range of $20\ ms$ to $10.24\ s$. To receive packets from advertising nodes, a scanning node listens to the three advertising channels in turn. The duration of time that the scanning node listens to an advertising channel is referred to as the *scan window* ($T_{scanWin}$). Scanning of the next advertising channel starts each *scan interval* ($T_{scanInt}$). The scanner node regularly scans the three advertising channels with a 100% duty cycle if the scan window and scan interval are set to be equal [20] [16].

C. BM Nodes Features

The BM protocol introduces four node features as *relay*, *friend*, *low power* and *proxy*. Such features can be enabled or disabled for each node.

Relay: A node with the relay feature receives data packets from its neighbors and forwards them to other nodes. Data packets may be sent from source to destination by relay-enabled nodes. Therefore, the relay feature plays a vital role in multi-hop mesh networking. Choosing relay nodes in a wise way is critical in BM networks [21], [22]. A low number of relay nodes in a BM network may lead to network disconnections, while an unnecessarily high number of relays may lead to packet collisions. Note that, in MBMNs, all nodes are assumed to be relay nodes.

Low power and Friend: A Low Power Node (LPN), which is intended for devices running on constrained energy sources (e.g., a small battery), is off for a large portion of time leading to decreased energy consumption. To avoid losing packets, each LPN has to associate with a Friend feature-enabled node (called Friend node). The latter receives and stores the LPN's packets in its buffer. LPNs periodically send a request poll to their Friend nodes asking for any packets in the Friend's buffer. The Friend nodes transfer the LPN's packets with a handshaking mechanism specified by the BM protocol [23]. Note that, in MBMNs, there are no LPNs, since all nodes are assumed to be able to act as relay nodes during their opportunistic participation in an MBMN.

Proxy: A node with proxy-enabled features forwards messages between the mesh network and non-BM BLE nodes, enabling the connection of BLE nodes to the BM network.

D. Multi-hop Mesh Networking

Multi-hop data transmission is realized using a controlled flooding mechanism in the network layer of the BM stack. In this mechanism, the relay nodes receive packets and forward them to all their neighbors [24]. To control the flooding and the level of redundancy in data packet transmission, two main mechanisms are used: cache, and Time-To-Live (TTL). Each relay node has a cache memory to store the source of packets and the last sequence number that this node has received from the source nodes. When a new packet is received, the node compares the sequence number of the received packet with the last sequence number saved in the cache for the corresponding source node. If the sequence number of the packet is equal to or smaller than the last saved sequence number, the packet is discarded. This mechanism prevents sending duplicate packets.

Each generated packet has a TTL counter assigned by its source node, which gets decreased by one unit by each relay node that receives the packet. A packet is forwarded in the network as long as its TTL is greater than one. Therefore, the number of hops that a packet can travel over the network is controlled. Proper setting of TTL by the source nodes is very important and has a direct impact on traffic load and thus network capacity. *Heartbeat* messages may be used in the protocol so that the source node can obtain an estimation of their hopwise distance to the desired destinations. The destination nodes may periodically flood the network with Heartbeat messages. When a source node receives a Heartbeat message from one of its desired destination nodes, it gets to know the number of hops the packet has traveled by subtraction of the primary packet's TTL and the current packet's TTL. The source nodes calculate the minimum and maximum number of hops to the destinations. Such values are used for setting proper TTL values when the source node generates packets. However, in MBMNs, the Heartbeat mechanism is not used, since mobility would render nodes' hopwise distance information useless.

Packet retransmissions may be activated in the network layer of the generator or relay nodes in order to raise the reliability of link-level packet delivery. These are controlled by two parameters, the *network transmit count* (N_{NTC}) and the *relay retransmit count* (N_{RRC}) in source and relay nodes, respectively. These parameters have a size of three bits and their values range from zero to seven. N_{NTC}=0 means only one transmission [25]. Retransmissions are separated in time by the network retransmit interval (T_{NreTx}) and the relay retransmit interval (T_{RreTx}) that are specified by two parameters, Network transmit interval steps ($Ntis$) and Relay retransmit interval steps ($Rris$). These parameters have a size of five bits and their values range from zero to thirty. Eqn. (1) and Eqn. (2) give these intervals as

$$T_{NreTx} = (Ntis + 1) \times 10ms + rand10 \tag{1}$$

$$T_{RreTx} = (Rris + 1) \times 10ms + rand10, \tag{2}$$

where $rand10$ is a random integer number in the range $[0,\ \ 10]$ ms. The minimum retransmission intervals should not be less than the minimum advertising interval, which is 20 ms.

III. Related work

Most studies about BM focus on static scenarios [9] [10], whereas mobile scenarios play a valuable role in IoT applications. This section gives a brief overview of such investigations with mobile scenarios. However, in these scenarios, most nodes are static, and the number of mobile nodes is limited. Networks in which all nodes are mobile have not been considered in the literature.

In [12], the capability and role of BM technology for infrastructure-less wireless connectivity for mobile robotic systems are explored. The study compares BM and other potential mesh technologies (for mobile robotic systems), including routing-based approaches and recent synchronous flooding techniques. According to this paper, BM natively supports mobility due to its managed flooding approach, which is transparent to topology changes caused by node mobility and does not require maintaining a network state regarding routing/forwarding tables. However, in their experimental evaluation, only four nodes are mobile, while most devices are static (20-25 static nodes).

In [13], BM networks are experimentally evaluated focusing on packet delivery performance. Twenty-nine fixed nodes, three mobile nodes, and one base station are deployed in an office environment. PDR and burst drop with different average hop distances for stationary and mobile nodes are evaluated. The authors indicated location and the number of relay nodes as effective parameters in the BM network's performance. They suggest that the BM technology is suitable for low packet generation rates because of its flooding mechanism. A high packet generation rate saturates relay nodes, having an inappropriate effect on PDR. This paper does not evaluate latency as a performance metric, and only three mobile nodes exist in its experiments. One of the significant results of these experiments is the PDR of the nodes in a specified area

This article has been accepted for publication in IEEE Sensors Journal. This is the author's version which has not been fully edited and
content may change prior to final publication. Citation information: DOI 10.1109/JSEN.2025.3545249

(Zone 2) being greater than 95% throughout every experiment, basically unaffected regardless of the mobile nodes' publish period.

In [14], the BLUEMERGENCY concept is explained. It is a practical solution for emergency networks based on mobile devices in a BM network. Two environments, a smart office, and a smart home, are used to evaluate the performance of BLUEMERGENCY. Two essential performance metrics used in these experiments are the response time to help requests and the packet loss rate. In these experiments, at most two mobile devices exist in each considered scenario. Furthermore, smartphones use the GATT bearer. Therefore, they do not participate in the packet flooding over advertising channels.

In [15] a mobile sink node (a smartphone or a similar portable device) collects sporadic data in a BM network. This work evaluates delivering data to a mobile sink node to increase energy efficiency. Moreover, it evaluates the global energy draw, the number of received packets, and the end-to-end delay. This work proposes two relay algorithms for routing data toward a mobile hub. However, they evaluate, by simulation, a static 50-node BM network with only one mobile sink node.

Previous research on BM networks has mainly focused on static networks or mobile networks with a limited number of mobile nodes. However, little attention has been paid to networks where all nodes are mobile. In this paper, we explore the concept of MBMN, where nodes are mobile, and evaluate their performance by means of simulation and by conducting experiments in a real mobile network in an outdoor environment.

IV. Studying the Performance of MBMNs

This section thoroughly examines the performance of MBMNs in a range of scenarios with different network sizes and node degrees, which represent the average number of neighbors a node has, utilizing the BM simulator (BMSim) developed in [26]. The investigations are categorized into three groups: network conditions, the ratio of packet generation interval to advertising interval, and retransmissions. The performance metrics of mobile networks can be affected by conditions that are distinct from those of static networks. In this section, we attempt to investigate and examine these conditions. As an example, the ratio between the packet generation interval and the advertising interval is observed to be an important factor that substantially influences the saturation of relay nodes. To better understand this phenomenon, various scenarios with different ratios are investigated. Furthermore, the effect of retransmissions in mobile networks is studied.

The challenges in mobile networks are illustrated through an example depicted in the Fig. 1. This figure illustrates the movements of nodes in a mobile network. The network comprises eleven nodes, and the deployment area is a square of $25\ m \times 25\ m$. Node movements were recorded over a four-second period, with each node moving 0.5 meters every second, using the random waypoint mobility model [27]. The first row of the figure displays the locations of the mobile nodes within the environment, while the second row illustrates the network topology based on the communication range of the nodes and their respective locations. Each topology and location picture was created after a one-second interval from the previous picture, during which each mobile node moved 0.5 meters.

TABLE I: Scenarios with different network sizes and densities [28]

Scenario size	Area ($m \times m$)	Node degree	Number of nodes
Small	25×25	7	11
Small	25×25	11	18
Small	25×25	15	24
Medium	50×50	7	44
Medium	50×50	11	69
Medium	50×50	15	94
Large	100×100	7	175
Large	100×100	11	275
Large	100×100	15	375
Very large	150×150	7	394
Very large	150×150	11	619
Very large	150×150	15	844

In Fig. 1a, node 6 is initially not a neighbor of nodes 3 and 4. After one second, node 6 moves 0.5 meters and is positioned within the communication range of nodes 3 and 4, as depicted in Fig. 1b. After another second, the distance between nodes 5 and 8 increases, causing them to go out of each other's communication range. Eventually, in Fig. 1c, the network is departed into two disconnected partitions. In Fig. 1d, despite the nodes' movements, the network topology remains disconnected. These figures illustrate significant changes in the topology of mobile networks that can lead to a disconnected topology or the creation of bottlenecks, making the investigation of these networks more complicated.

This section will initially cover the overall setup of the simulations that were conducted, and subsequently provide the results and an in-depth analysis of our observations.

A. Simulation setup

The evaluated scenarios correspond to mobile nodes distributed over a square-shaped area, with a wide range of topologies (see Table I), as described in [28]. The mobility model utilized is a random waypoint model, with each node moving at a speed uniformly randomly selected from the range of $0.25\ m/s$ to $1\ m/s$ and a mobility step of 1 second indicates that the network nodes move, and the network topology changes every second. This speed range corresponds to the human walk. The communication range for all nodes is set to 11.26 meters, resulting in average node degrees of 7, 11, and 15 for networks of different sizes and environment areas, as presented in Table I. Take into consideration that the average node degrees, which represent the average number of neighbors per node, were selected as a baseline from another study (i.e., [28]), where the scenarios were static (i.e., nodes had no mobility). Mobility may introduce deviations in the node degree, depending on the mobility model. In order to better isolate the phenomena that affect network performance, it is assumed that all links have a perfect packet reception ratio of 100%. As a result, no packets are lost due to channel

This article has been accepted for publication in IEEE Sensors Journal. This is the author's version which has not been fully edited and
content may change prior to final publication. Citation information: DOI 10.1109/JSEN.2025.3545249

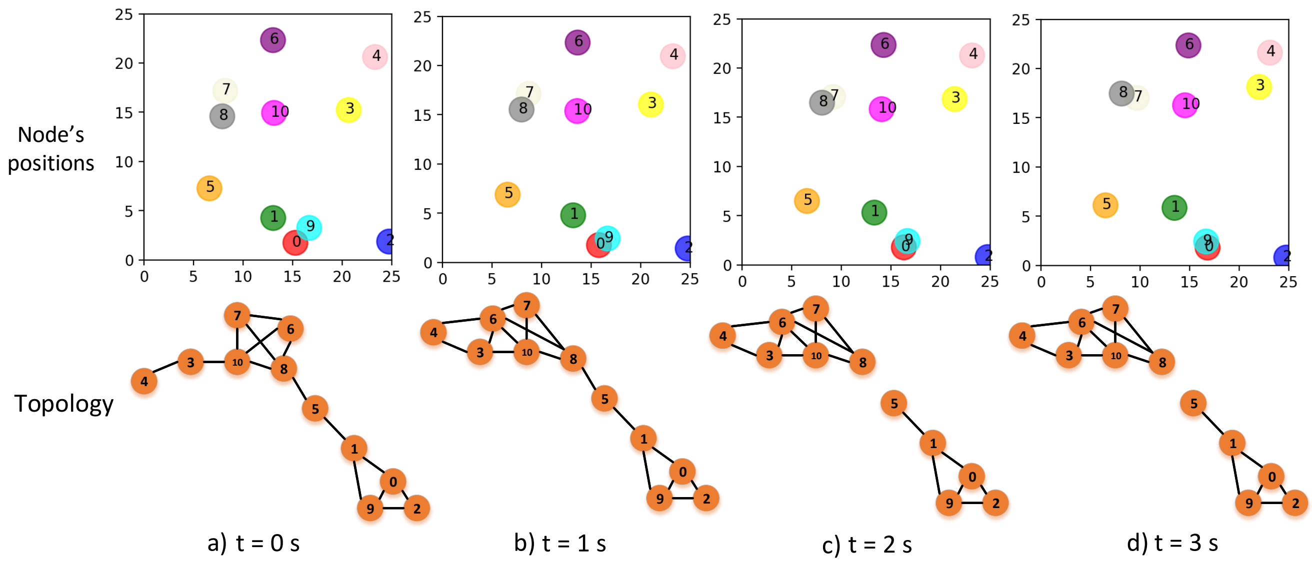

Fig. 1: Illustration of nodes' location and the resulting topologies at four snapshots of a network spaced by one second. All nodes move with a speed of $0.5\ m/s$.

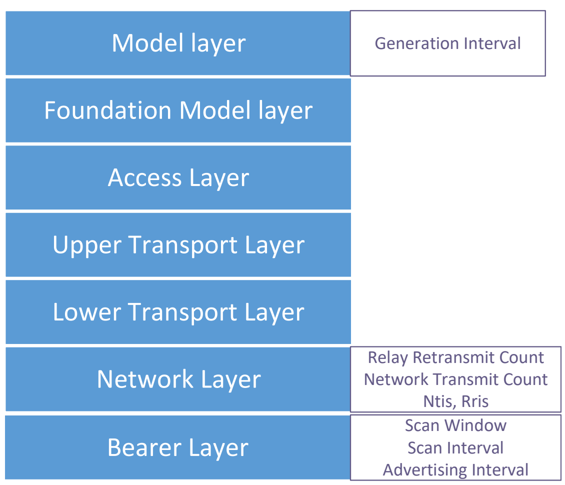

Fig. 2: BM protocol stack with evaluated parameters across different layers [16]

effects such as multi-path fading or external interference when nodes are within each other's communication range. In each scenario, a randomly chosen node is designated as the sink for data packets. The sink node is considered to be mobile like the other nodes. All nodes have the relay feature enabled to minimize node isolation. Additionally, all nodes generate packets at a specific interval (T_{gen}). The buffer size for each node is set to 6, allowing relay nodes to store up to 6 packets from other nodes for relaying. The simulation time, defined as the duration of a single simulation in a given scenario, is 10 minutes. Table II displays the common parameters used in all simulation scenarios and indicates the corresponding protocol stack layers for each parameter. In addition, Fig. 2 illustrates the BM protocol stack, highlighting the specific protocol parameters evaluated at each layer.

The performance metrics considered for the evaluation include the PDR, the average latency of delivered data packets per node in the network, the average number of hops traveled by the received packets, and the number of transmissions and collisions in the network. The deployment area size for networks with different sizes is indicated on the horizontal axis in most of the plots, which are presented as boxplots to illustrate the statistical features of their distributions. For each horizontal axis value, the central box contains 50% of the data points, representing the two middle quartiles, as well as the median. The upper and lower whiskers extend from the top and bottom of the box, respectively, positioned at a distance of 1.5 times the length of the box, from the upper and lower box edges. Data points that fall outside the whiskers are considered outliers and are represented as black circles. The blue, red, and green boxplots correspond to networks with node degrees 7, 11, and 15, respectively. The scenarios are simulated 10 times, except for the scenarios with 615 and 844 nodes, which are simulated 5 times (due to the very high execution time for such large networks). These simulations are conducted using different seeds to ensure more statistically reliable results.

B. Results and discussion

This section focuses on the comprehensive analysis of four main performance metrics in MBMNs: the PDR, the average latency of delivered data packets per node, the average number of hops traveled by received packets, and the number of transmissions and collisions. These metrics are thoroughly examined across different network sizes to provide a comprehensive understanding of MBMN performance. Additionally, a detailed comparison between static networks and MBMNs is provided to highlight the distinctive capabilities of MBMNs. In the following, the results are discussed from three angles. First, the performance in various conditions of the network (size

This article has been accepted for publication in IEEE Sensors Journal. This is the author's version which has not been fully edited and content may change prior to final publication. Citation information: DOI 10.1109/JSEN.2025.3545249

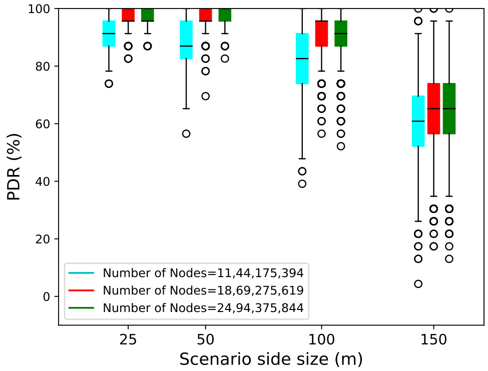

(a) End-to-end packet delivery ratio (PDR)

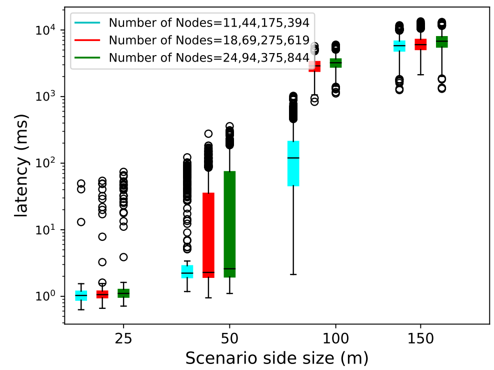

(b) Latency of delivered data packets

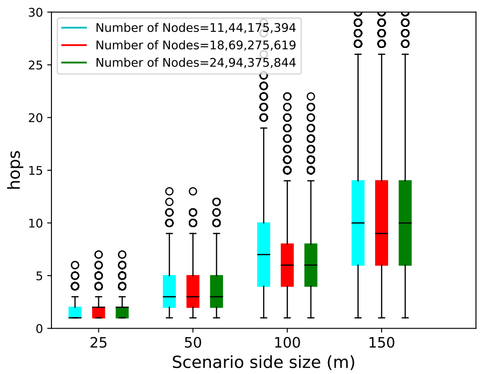

(c) Average number of hops traveled by received packets

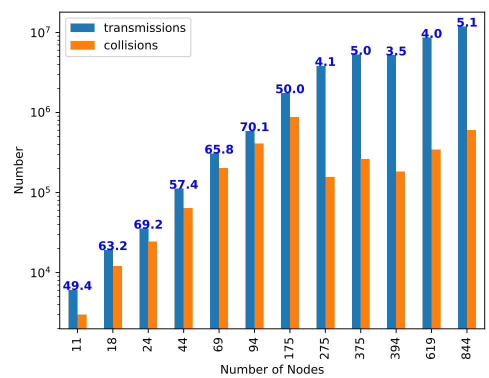

(d) Number and percentage of collisions. The percentage of collisions is shown at the top of each column bar.

Fig. 3: Performance results for MBMNs with T_{gen} = 25000 ms and T_{adv} = 120 ms

TABLE II: Default settings in evaluated scenarios

BM Stack Layer	Parameter	Value
Bearer layer	Scan Window	30 ms
Bearer layer	Scan Interval	30 ms
Bearer layer	Advertising Interval	per scenario
Network layer	Ntis	1
Network layer	Rris	1
Network layer	Relay Retransmit Count	0
Network layer	Network Transmit Count	0
Network layer	Heartbeat Mechanism	OFF
Application	Generation Interval	per scenario
-	Packet Reception Ratio	100%
-	Communication Range	11.26
-	Simulation Time	600000 ms
-	Buffer Size	6
-	Mobility Step	1000 ms
-	Mobility Speed Distribution	[0.25, 1] m/s
-	Relay Nodes	All nodes
-	Generator (source) Nodes	All nodes

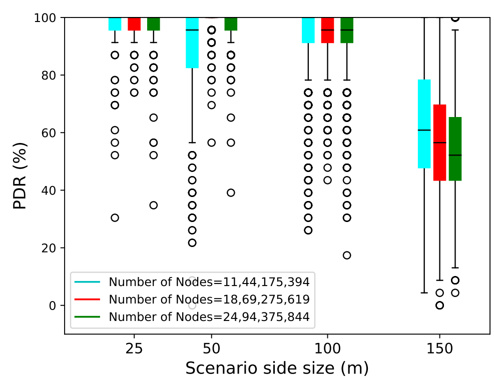

Fig. 4: PDR in networks with T_{gen} = 25000 ms T_{adv} = 120 ms and speed = 0 m/s

and density) is analyzed. Then the impact of advertising and generation interval and the number of packet retransmissions are discussed.

1) Network size and density: Fig. 3 shows results for MBMNs where the generation interval and advertising interval are set to $T_{gen} = 25000\ ms$ and $T_{adv} = 120\ ms$, while the other parameters are set to their default values. In Fig. 3a, it can be observed that the networks with a node degree of 7 (represented by the blue boxplot) have a lower PDR compared to networks with degrees of 11 and 15. This is because the number of nodes in the network is relatively low compared to the size of the environment, which increases the likelihood of the network becoming disconnected or some nodes becoming bottlenecks in the network, as the nodes move around. Also, for a given node density, PDR tends to decrease for a higher size of the area, offering generally high PDR (e.g., greater

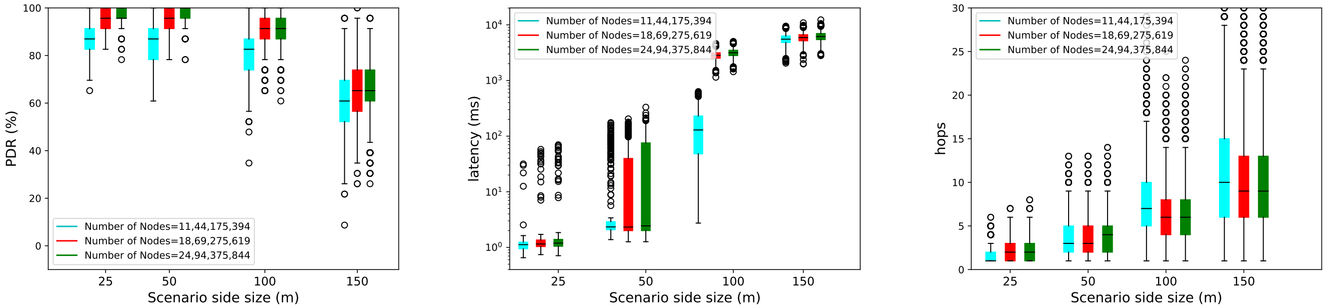

(a) mobility speeds = Up to 5 m/s (b) mobility speeds = Up to 5 m/s (c) mobility speeds = Up to 5 m/s

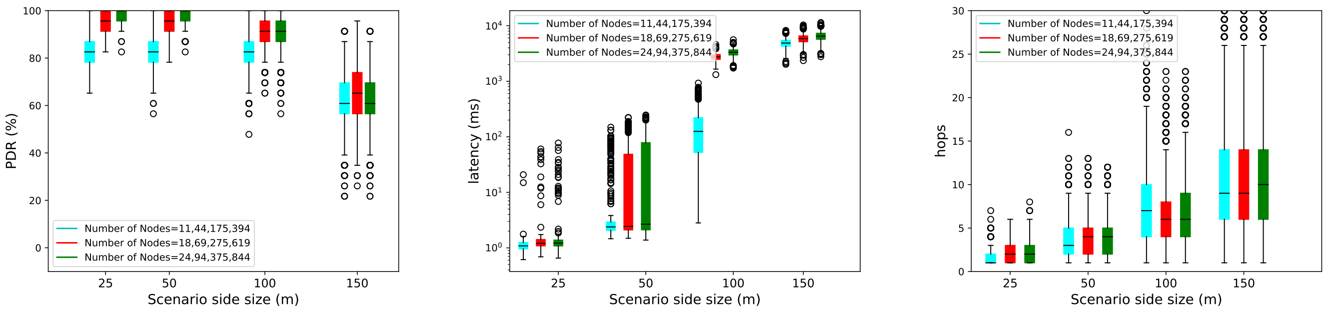

(d) mobility speeds = Up to 10 m/s (e) mobility speeds = Up to 10 m/s (f) mobility speeds = Up to 10 m/s

Fig. 5: PDR, latency and hop distance in networks with different mobility speeds

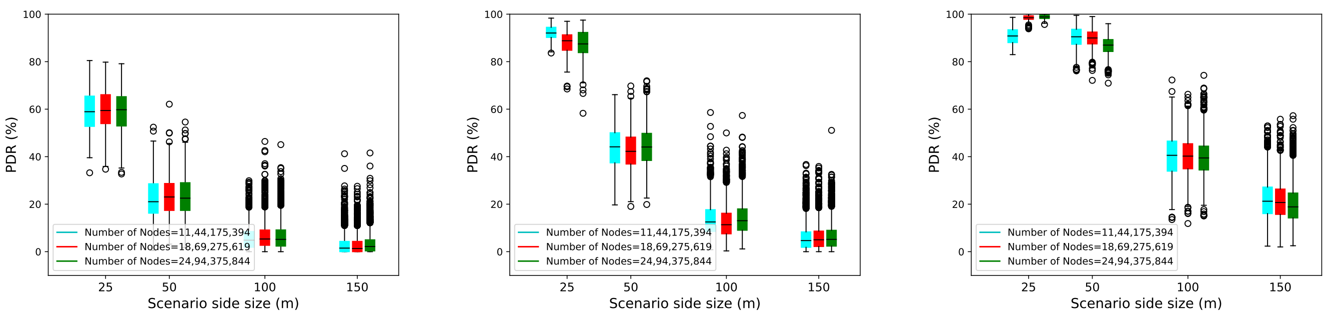

(a) T_{gen} = 1000 ms T_{adv} = 500 ms (b) T_{gen} = 1000 ms T_{adv} = 120 ms (c) T_{gen} = 1000 ms T_{adv} = 20 ms

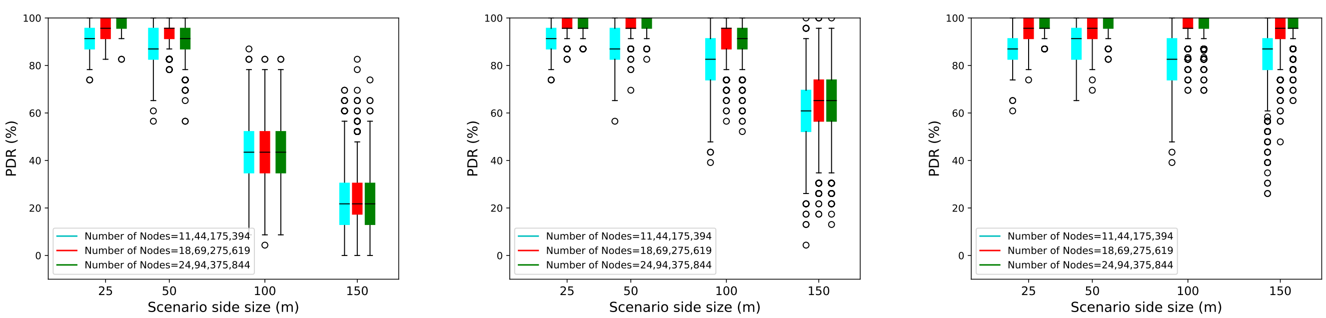

(d) T_{gen} = 25000 ms T_{adv} = 500 ms (e) T_{gen} = 25000 ms T_{adv} = 120 ms (f) T_{gen} = 25000 ms T_{adv} = 20 ms

Fig. 6: PDR in different networks with different generation and advertising intervals

than 80% for an area of $100\ m \times 100\ m$).

Latency is mainly affected by the hop distance between the source and destination nodes. In Fig. 3b, the latency in each environment size is shown to increase as the scenario size grows, with similar values for a given scenario size across different node degrees. This is largely due to the average number of hops traveled by received packets, as indicated in Fig. 3c, which also shows similar values across different

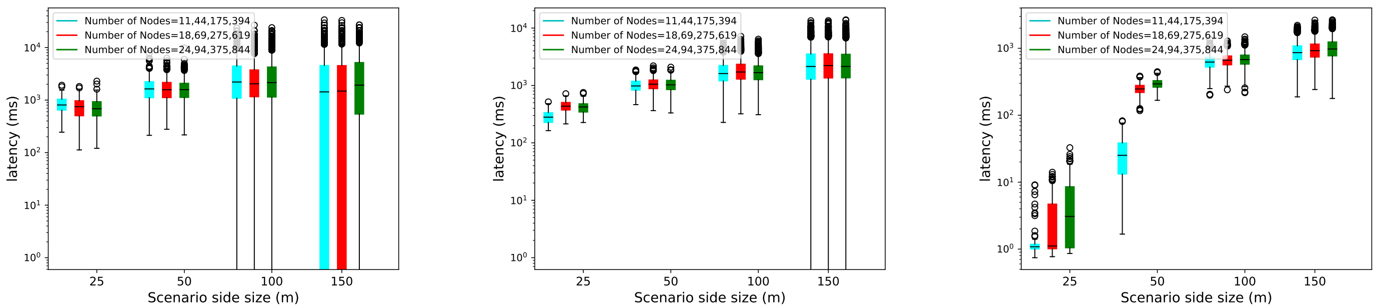

(a) T_{gen} = 1000 ms T_{adv} = 500 ms (b) T_{gen} = 1000 ms T_{adv} = 120 ms (c) T_{gen} = 1000 ms T_{adv} = 20 ms

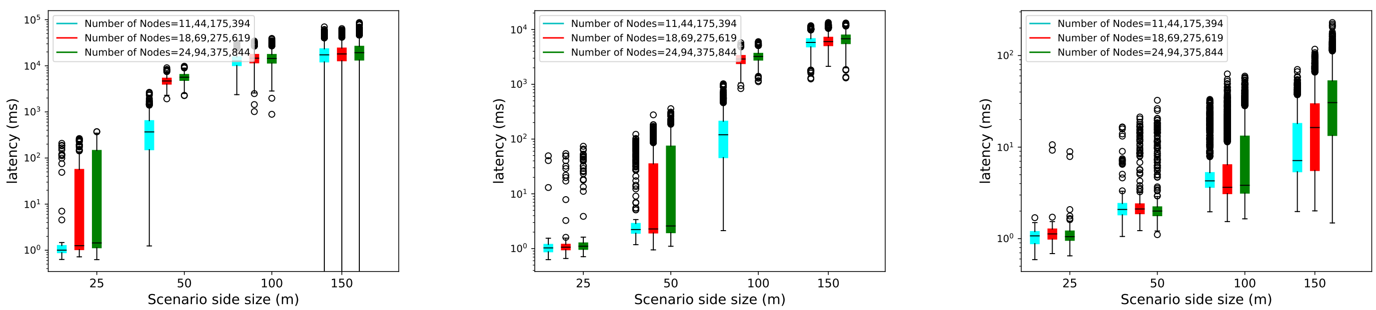

(d) T_{gen} = 25000 ms T_{adv} = 500 ms (e) T_{gen} = 25000 ms T_{adv} = 120 ms (f) T_{gen} = 25000 ms T_{adv} = 20 ms

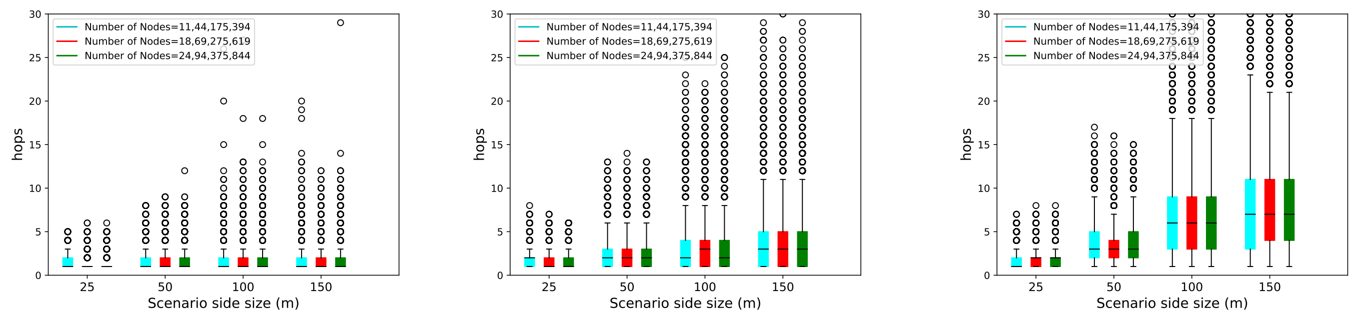

(g) T_{gen} = 1000 ms T_{adv} = 500 ms (h) T_{gen} = 1000 ms T_{adv} = 120 ms (i) T_{gen} = 1000 ms T_{adv} = 20 ms

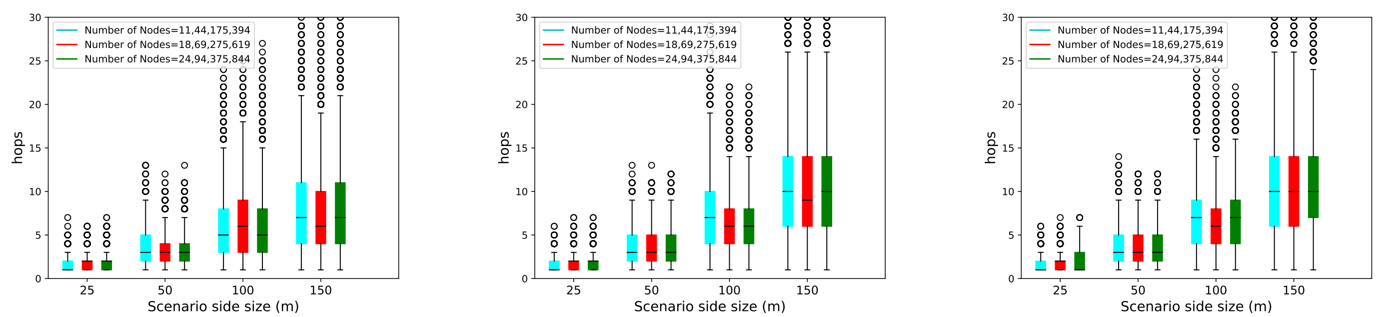

(j) T_{gen} = 25000 ms T_{adv} = 500 ms (k) T_{gen} = 25000 ms T_{adv} = 120 ms (l) T_{gen} = 25000 ms T_{adv} = 20 ms

Fig. 7: Latency and hop distance in different networks with different generation and advertising intervals

scenario sizes, and increases with scenario size. Moreover, the impact of saturated relay nodes on latency is evident in Fig. 3b, with networks containing more than 175 nodes exhibiting a significant increase in latency. This can be attributed to the fact that packets stay in the buffer of saturated relay nodes for a longer time, contributing to the observed latency increase.

In Fig. 3c, the average number of hops traveled by the received packets in each mobile network is presented. These values are relatively similar for each scenario size. The number of traveled hops is mainly affected by the scenario size and node range, rather than the number of nodes. However, the latter plays a critical role in creating a connected network.

The average number of hops traveled by received packets has a significant impact on the PDR and latency. When the hop distance is greater, there are more relay nodes along the path between the source and destination, which increases the likelihood of packet loss in their buffers and decreases the PDR. Additionally, packets may stay in the buffers of relay nodes for longer periods, resulting in increased latency. Comparing Fig. 3a and Fig. 3c reveals that as the average number of hops traveled by received packets increases, the PDR decreases. Furthermore, the PDR values in each scenario are similar for different numbers of nodes due to the similar values in the average number of hops traveled by received packets.

In Fig. 3d, the number of transmissions and collisions in the considered MBMNs are presented. The number of nodes in the networks is specified on the horizontal axis, and the percentage of collisions is shown at the top of each column bar. As shown in this figure, the collision percentage drops significantly in the networks with a number of nodes greater than 175. This is due to an increase in the number of source nodes, leading to a higher load in the network and saturated relay nodes in some parts of the network. Consequently, the saturated relay nodes can not save new packets in their buffers so these packets are lost and cannot reach the relay nodes closer to the sink node. As a result, the number of new packets in the relay nodes closer to the sink node decreases, leading to a reduction in the number of transmissions by the relay nodes and, consequently, fewer collisions. Additionally, because all nodes in the network are generator nodes, the number of transmissions is high, which also contributes to the decrease in the percentage of collisions.

2) Mobility: To evaluate the impact of different node speeds in the BM network, a series of experiments were conducted with varying maximum node speeds: 0 m/s, 1 m/s, 5 m/s, and 10 m/s. The results of these experiments are presented in Fig. 4, Fig. 3 and Fig. 5.

Fig. 4 presents simulation results from a scenario where nodes did not move (i.e. had a speed of 0 m/s). Upon comparing the PDR values in Fig. 4 and Fig. 3a, that has mobility speed up to 1 m/s. it is evident that certain networks experienced a significant increase in PDR, while others demonstrated a decrease. In static networks, the PDR is greatly influenced by the network topology. For example, if specific networks are free of bottlenecks or congestion, like in networks with 18, 24, 69, and 94 nodes, the PDR increases. However, if there is congestion on a particular node, as in some of the networks with 44 nodes, the PDR significantly decreases as there is no chance of topology changes without mobility. In contrast, in mobile networks, where the topology keeps changing due to mobility, the network's topology at a given instance does not cause any significant impact on overall PDR.

The experiments with node speeds of up to 1, 5, and 10 m/s, as presented in Fig. 3 and Fig. 5, show similar results. It is important to note that while 1 m/s is a realistic speed for human mobility (approximately walking pace), the greater speeds of 5 and 10 m/s are not common for pedestrian mobility. These higher speeds were included in the experiments primarily to explore how increased mobility might affect network performance and to assess the BM network's adaptability to varying degrees of motion. The results indicate that even at these elevated speeds, The network's performance remains relatively consistent, indicating that the BM network design can handle moderate to high mobility without degradation in PDR and latency. This suggests that the flooding mechanism in BM networks is effective in maintaining message delivery in mobile environments, making it a suitable choice for applications involving node movement.

3) Ratio of packet generation and advertising intervals: We investigate the impact of the ratio between the generation and advertising intervals in MBMNs in terms of PDR (Fig. 6), as well as latency and number of hops (Fig. 7). This ratio has a significant influence on the creation of saturated relay nodes with full relay buffers, resulting in a PDR decrease. In Fig. 6a, the generation and advertising intervals are 1000 and 500 ms, respectively. In this case, the advertising interval is relatively high compared to the generation interval. As a result, packets stay in the buffer of relay nodes for a longer time, causing the buffer to become full. Eventually, the relay nodes discard new packets, and the destination node misses most of the packets due to the path with saturated relay nodes. Also, in Fig. 7g, we observe that the received packets traverse only a few hops, indicating that they originate from nodes near the sink node. Conversely, packets from nodes far away from the sink node fail to reach their destination due to a path congested with saturated relay nodes. This observation is confirmed by the latency depicted in Fig. 7a. Despite an advertising interval of 500 ms causing a low exit rate in the relay nodes' buffer, the latency remains relatively low. This is because the received packets primarily come from nodes near the sink, while other packets are lost along the lengthy path with saturated relay nodes.

In Fig. 6b, the advertising interval is reduced to 120 ms, leading to a higher exit rate from the buffer of relay nodes and an increase in PDR in comparison to Fig. 6a. However, this enhancement is more noticeable in small networks, as opposed to large networks where relay nodes may become saturated. Comparing Fig. 7h with Fig. 7g, as well as Fig. 7b with Fig. 7a, reveals a low disparity between networks with advertising intervals of 500 ms and 120 ms. Both scenarios depict saturated relay nodes along the network paths, resulting in packets from distant nodes unable to reach the sink node consistently. Consequently, the number of hops traveled by delivered packets remains low, leading to low latency despite the low exit rate from buffer nodes. The advertising interval is further decreased to 20 ms, resulting in an overall increase in PDR across all networks as shown in Fig. 6c. In these networks, as illustrated in Fig. 7i, the average number of hops traveled by packets is increased indicating successful reception of packets from nodes distant to the sink node. Furthermore, the high exit rate from relay node buffers reduces latency in small networks. However, as shown in Fig. 7c, a sharp rise in latency is observed between the 44-node and 69-node networks, highlighting the prevalence of saturated relay nodes within the paths of larger networks.

Fig. 6d, Fig. 6e, and Fig. 6f further investigate the impact of the ratio between generation and advertising intervals

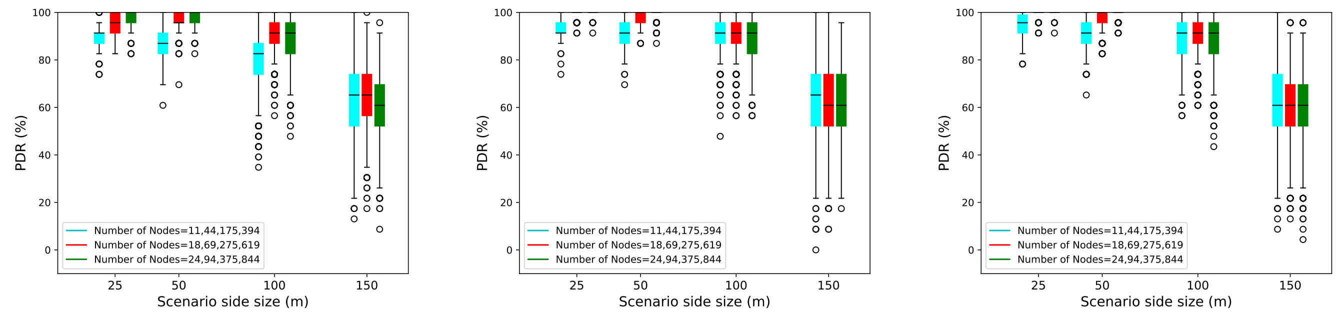

(a) N_{NTC} = 0 and N_{RRC} = 0 (b) N_{NTC} = 1 and N_{RRC} = 1 (c) N_{NTC} = 2 and N_{RRC} = 2

Fig. 8: PDR in different networks with different retransmission settings

in networks with the generation interval of 25000 ms and changing the advertising interval to 500, 120, and 20 ms, respectively. Since the generation rate is low, there are almost no collisions in these networks, and the impact of filled buffers of relay nodes is clearly visible in those cases where the PDR is not high. A comparison between figures Fig. 6d and Fig. 6e shows that the three large networks with 175, 275, and 375 nodes have a significant improvement in their PDR when the advertising interval is reduced to 120 ms. Similarly, a comparison between Fig. 6d, Fig. 6e, and Fig. 6f indicates that the three very large networks with 394, 619, and 844 nodes experience a substantial increase in their PDR when the advertising interval is set to 20 ms. Upon examining Fig. 7j, Fig. 7k, and Fig. 7l it becomes apparent that networks with a generation interval of 25,000 ms and an advertising interval of 20 ms exhibit a higher average number of hops traveled by received packets. This phenomenon occurs because these networks lack saturated relay nodes in their paths, enabling the reception of packets from nodes far from the sink node. Conversely, in networks with advertising intervals of 500 and 120 ms, packets originating from distant nodes are unable to traverse the extended path due to congestion caused by saturated relay nodes. In terms of latency, by comparing Fig. 7d, Fig. 7e, and Fig. 7f, it is evident that as the advertising interval increases, latency also increases. This is due to the formation of saturated relay nodes leading to packets staying in the buffer of these saturated relay nodes for a long period. Additionally, Fig. 7d and Fig. 7e, highlight a sharp rise in latency as the number of nodes increases, illustrating the emergence of saturated relay nodes in larger networks.

When comparing scenarios with generation interval of 1000 ms to those with generation interval of 25000 ms, it becomes evident that the ratio between the generation and advertising intervals in the latter is greater than in the former. Consequently, the PDR in Figures 6d, 6e, and 6f is higher than in Figures 6a, 6b, and 6c. However, due to the lower generation and advertising intervals in scenarios with generation interval of 1000 ms, collisions are more frequent in these networks compared to scenarios with generation interval of 25000 ms. This suggests that maintaining a greater ratio between the generation and advertising intervals has a more positive impact on PDR, as it leads to a reduction in the number of saturated relay nodes.

4) Retransmissions: To improve the reliability of the BM network, packet retransmissions can be enabled at the network layer of both generator and relay nodes. However, in MBMNs, the distance between nodes varies, and the number of neighboring nodes fluctuates over time, potentially impacting the PDR. Therefore, this section focuses on investigating the influence of increasing retransmissions in relay and source nodes on the reliability of MBMNs. The aim is to understand how adjusting the retransmission parameters can enhance the overall reliability of the network.

In Fig. 8, similar network configurations to those in Fig. 3 are considered. In Fig. 8b, increasing the number of retransmissions by one for relay and generator nodes improves the PDR in Small and Medium scenarios resulting in networks containing 18, 24, and 94 nodes achieving a PDR of 100%. However, in Large and Very Large scenarios, increasing the number of retransmissions can have a counterproductive effect as it leads to collisions and an increase in saturated relay nodes. In Fig. 8c, the number of retransmissions per generator and relay node is tripled. Comparing Fig. 8b and Fig. 8c shows that there is no significant difference between them (PDR decreased in some cases). This is due to a higher number of collisions and congestion caused by the increased retransmissions, as well as reduced scanning time for relay nodes. Therefore, determining the optimal number of retransmissions for relay and generator nodes requires careful consideration as it can have either a positive or negative impact on PDR, which depends on the conditions of specific scenarios.

V. MBMNs in a Real Environment

The previous section investigated the impact of various parameters and conditions on the performance of MBMNs by simulating different scenarios. In addition, this section provides a real-life implementation of an MBMN in an outdoor field. In these experiments, nodes were carried by people (each person was given a node) who move around the field, with two different deployment areas of size $40m \times 40m$ and $25m \times 25m$, both with a square shape. These deployments can serve as examples for various outdoor applications. As the walking speed of humans typically ranges from 0 to ~1 m/s, we requested participants to maintain a speed close to the middle

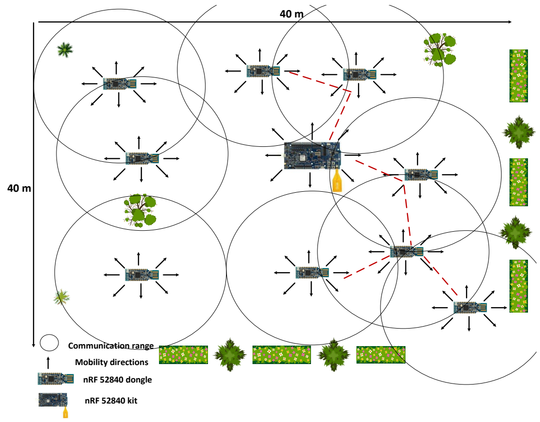

Fig. 9: Mobility of BM nodes in an outdoor environment

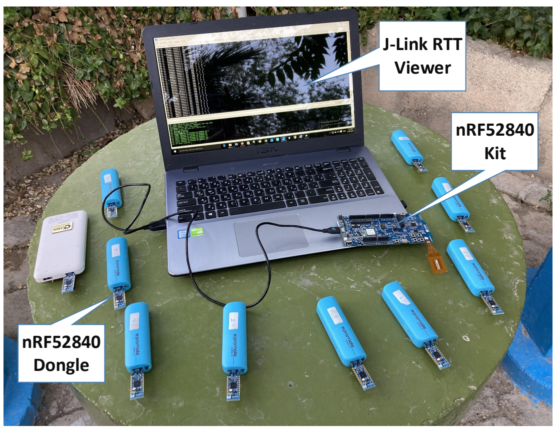

Fig. 10: The setup for the real experiments consisted of hardware and software arranged on a tabletop

of this range, approximately 0.5 m/s. The mobile network consists of 11 mobile nodes including the sink node. Fig. 9 illustrates a snapshot of such deployment area, the directions of movement, and the communication range of nodes. Based on the communication range and nodes' movement, the mobile network in Fig. 9 can either be fully or partially connected.

The setup for the experiments is shown in Fig. 10, which consisted of both hardware and software components. The Nordic Semiconductors PCA10056 development kit and PCA10059 dongles, both equipped with the nRF52840 chipset, were used in the experiments. These devices have a receiver sensitivity of -95 dBm in 1 Mbps data rate. Also, transmit power is set to 0 dBm. The SEGGER Embedded Studio was used to program the PCA10056 kit while the Nordic Semiconductor nRF Connect was used to program the PCA10059 dongles. The nodes were provisioned and configured with the help of a smartphone using the nRF mesh Android App [29].

A total of 10 PCA10059 dongles were programmed with the light switch server firmware, and one PCA10056 kit was programmed with the light switch client firmware. The light switch server nodes transmitted packets to the light switch client node periodically every 1000 ms (T_{gen} = 1000). The network transmit count was 0, and *Ntis* had a value of 1. All server nodes had an active relay feature with a relay retransmit count of 0 and *Rris* value of 1. In these experiments, the Heartbeat mechanism is disabled, and the initial TTL of packets is configured to 10. The light switch client node was connected to a PC, which received packets from all server nodes. The source ID, sequence number, and TTL of every received packet were sent to the computer and stored in a log file using the J-link RTT viewer software. The log file was used to post-process the received packets and calculate the PDR and traveled hop count for each server node.

We first conducted an experiment using two nodes (a sender and a receiver) in our outdoor environment to determine the communication range of the devices. In this experiment, all packets were received by the receiver when the distance is up to 8 meters. Packet loss occurred within the range of 8 to 15 meters. However, the actual link quality can be affected by various factors, such as the device's orientation, altitude, and environmental conditions. The results vary across the performed experiments.

Due to the characteristics of the deployment environment, multi-hop data delivery to the client node (i.e., sink node) connected to the computer is often necessary. The experiments have a duration of approximately 10 minutes. After the experiments conclude, the log file is analyzed to extract the PDR and the number of hops traveled by the packets received at the destination. The top row of Fig. 11 displays the results of an experiment conducted in a $25m \times 25m$ environment with 11 nodes, which is similar to the Small scenario described in Section IV (see Table I). The environment size was then increased to $40m \times 40m$ with the same node configuration (see the results at the bottom row of Fig. 11).

Fig. 11a and Fig. 11d display the PDR from each mobile node in the $25m \times 25m$ and $40m \times 40m$ environments, respectively. It can be observed that the PDR decreases as the environment size increases, although it remains at relatively high values in the considered scenarios, generally greater than 90%. Additionally, Fig. 11b and Fig. 11e depict the average number of hops traveled by the received packets for each source node. The average hop distance is similar for all nodes, as a result of the random movement of nodes. As expected, it is slightly greater in the $40m \times 40m$ scenario. The average hop distance does not significantly impact the PDR, except in specific cases where the number of hops increases (e.g., node 5 in Fig. 11d and Fig. 11e). In these scenarios, the number of nodes remains constant as the dimensions of the environment increase. This implies that the number of source nodes does not increase, resulting in no saturated relay nodes in network paths affecting the PDR. Fig. 11c and Fig. 11f illustrate the PDR and the number of hops taken by received packets over time for nodes 4 and 5 in environments of $25m \times 25m$ and $40m \times 40m$, respectively. The horizontal axis of the plots represents the sequence number of packets generated by the mobile nodes. The PDR values are based on the recent packet delivery estimate over the last 30 sequence numbers. As shown in Fig. 11f, the number of hops taken by received packets in node 5, which has the lowest PDR among all the conducted experiments, varies between 1 and 6 (with values of 4 being the most frequent one) while in Fig. 11c for node 4, it is mostly limited to values of 1 or 2.

This article has been accepted for publication in IEEE Sensors Journal. This is the author's version which has not been fully edited and
content may change prior to final publication. Citation information: DOI 10.1109/JSEN.2025.3545249

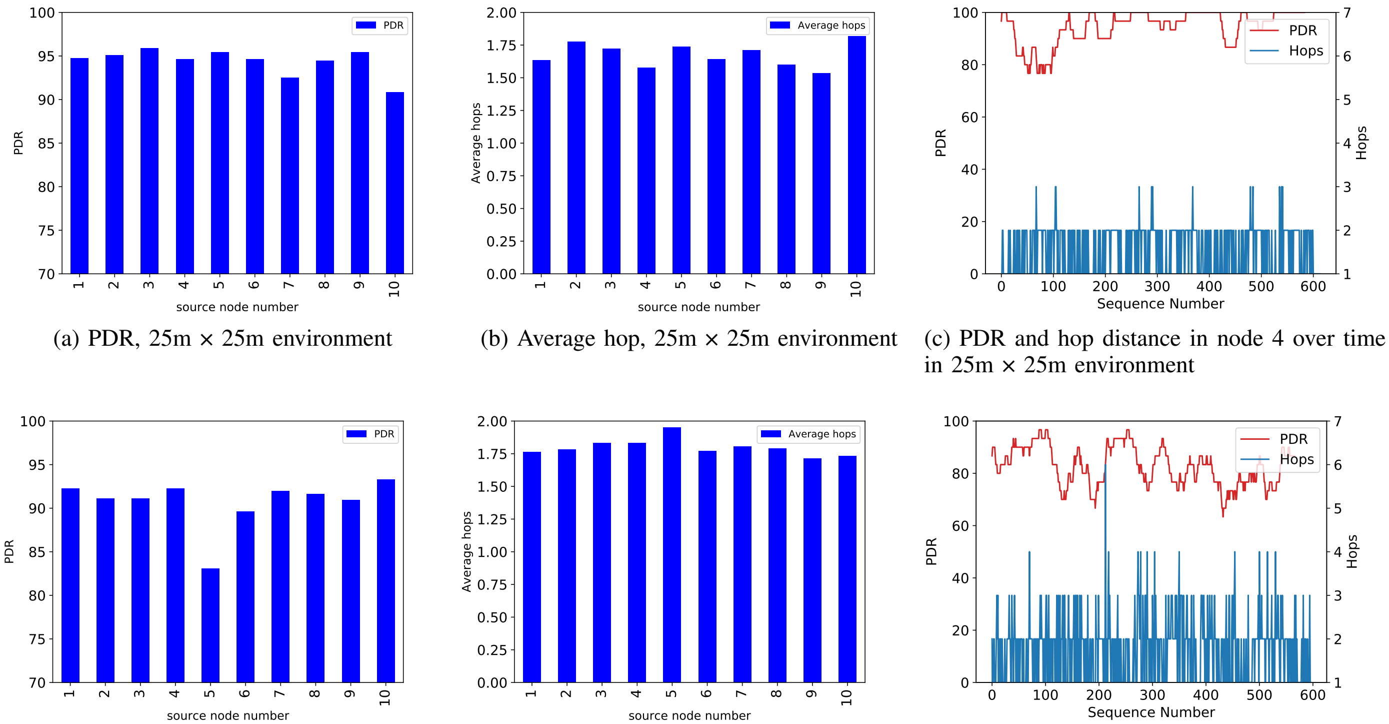

(a) PDR, 25m × 25m environment
(b) Average hop, 25m × 25m environment
(c) PDR and hop distance in node 4 over time in 25m × 25m environment
(d) PDR, 40m × 40m environment
(e) Average hop, 40m × 40m environment
(f) PDR and hop distance in node 5 over time in 40m × 40m environment

Fig. 11: PDR and hop distance of mobile nodes in an outdoor environment

VI. Limitations of the Study

This study provides valuable insights into the performance of MBMNs under various conditions; however, there are certain limitations to both the simulation and experimental evaluations that should be considered. These limitations may be the subject of future research in MBMNs.

A. Simulation Limitations

Mobility Model: The simulations utilized a random waypoint mobility model with node speeds ranging between 0.25 and 10 m/s, with a mobility step of 1 second (i.e., nodes move every second). While this model provides a useful baseline, it is just one of many potential mobility models. Other models with different speeds, movement patterns, and update intervals [30] [31] were not explored.

Node Configurations: Each node in a Bluetooth Mesh network has multiple configurable parameters and mechanisms across various layers. In our simulations, we focused on important parameters such as the Relay Retransmit Count, Network Transmit Count, Advertising Interval, and Packet Generation Interval. However, other potential configurations were not investigated, which could influence the overall network performance.

Network Conditions: The study examined different networks with varying conditions, including different numbers of nodes, environment dimensions, and node degrees. Although these scenarios provide diverse perspectives, they do not encompass all possible network setups. The simulations did not reflect some real-world phenomena such as interference from non-Bluetooth devices, physical obstacles, or variable environmental conditions.

Performance Metrics: We evaluated network performance using metrics such as PDR, latency, hop distance, and collision percentage. While these metrics offer valuable insights, they do not cover the full range of possible performance indicators, such as energy consumption or memory usage of the devices.

B. Real Experiments Limitations

Device Limitations: The experiments were conducted using a network of 11 Bluetooth Mesh devices, which represents a constraint on the network size. Larger-scale networks were not tested. We were only able to test two environments with dimensions of 25×25 meters and 40×40 meters. While these provide a basic understanding of performance in confined spaces, more varied environmental conditions were not explored.

Performance Metrics: In our experimental setup, we focused on evaluating key metrics such as PDR, average hop count, and the behavior of these metrics over time. Other potential performance indicators were not measured.

Mobility Model: The experiments used a single mobility model, where all nodes moved at an average speed of approximately 0.5 m/s, aiming to capture human walking speed. This uniform mobility scenario limits the exploration of networks with more dynamic or heterogeneous mobility patterns.

VII. Conclusions

BM offers a protocol that enables scalable networking of IoT devices using the widely utilized BLE technology. While previous research on BM networks has primarily focused on static networks or limited mobile networks, this paper introduces and assesses the performance of MBMNs. MBMNs can be opportunistically established in diverse environments for various purposes. This study investigates three important factors in these networks: the unique characteristics of mobile networks compared to static networks, the impact of the generation-to-advertising interval ratio on the saturation of relay nodes, and the effects of retransmission, over a wide range of scenarios. The study also analyzes the influence of the considered main factors and the stemming network topology features, and their impact on performance. The performance metrics of real mobile networks in an outdoor environment are evaluated to demonstrate the feasibility and relatively good performance of MBMNs.

The results obtained from the conducted study affirm the feasibility of MBMNs with satisfactory performance in many scenarios. Additionally, MBMNs offer an advantage over static networks by eliminating the influence of a sometimes inadequate network topology on the PDR. However, it is worth noting that in MBMNs, the ratio of packet generation and advertising intervals plays a crucial role and can lead to the presence of saturated relay nodes in larger networks, which poses limitations to network scalability. Furthermore, the selection of retransmission-related parameter values needs to be carefully considered. As shown in this paper, BM is practical with default settings in a range of scenarios. However, trade-offs arise (e.g. with the number of retransmissions), suggesting that careful parameter configuration needs to be considered for a given scenario. This study illustrates the achievable performance of MBMNs in a diversity of scenarios, thus providing valuable information for researchers, engineers and developers.

We next provide ideas for future work in the novel field of MBMNs. In our experiments, all network nodes were considered as smartphones, assuming no energy consumption constraints. As a result, all nodes functioned as relay and generator nodes. However, investigating MBMN performance in networks that include friend nodes and low-power nodes would be highly valuable, especially for IoT applications, where the use of energy-constrained devices as relay nodes may be limited. Additionally, due to mobility in MBMNs, we disabled Heartbeat messages. However, without Heartbeat message transmission, the network TTL remains at its default high value (127). Developing a mechanism to dynamically adjust TTL based on node distance and mobility—without introducing excessive overhead—could be a challenging research topic.

VIII. Acknowledgment

This work was partly supported by the SCOTT European project that has received funding from the Electronic Component Systems for European Leadership Joint Undertaking under grant agreement No737422. Carles Gomez was funded in part by the Spanish MCIU/AEI/10.13039/501100011033/FEDER/UE through project PID2023-146378NB-I00, and by Secretaria d'Universitats i Recerca del departament d'Empresa i Coneixement de la Generalitat de Catalunya with the grant number 2021 SGR 00330.

References

[1] "2023 bluetooth market update." [Online]. Available: https://www.bluetooth.com/blog/now-available-new-bluetooth-forecasts-and-trends

[2] I. Natgunanathan, N. Fernando, S. W. Loke, and C. Weerasuriya, "Bluetooth low energy mesh: Applications, considerations and current state-of-the-art," *Sensors*, vol. 23, no. 4, p. 1826, 2023.

[3] J. F. Ensworth and M. S. Reynolds, "Ble-backscatter: Ultralow-power iot nodes compatible with bluetooth 4.0 low energy (ble) smartphones and tablets," *IEEE Transactions on Microwave Theory and Techniques*, vol. 65, no. 9, pp. 3360–3368, 2017.

[4] S. M. Darroudi and C. Gomez, "Bluetooth low energy mesh networks: A survey," *Sensors*, vol. 17, no. 7, p. 1467, 2017.

[5] S. Bluetooth, "Mesh profile specification: 1.0," *Bluetooth Special Interest Group: Kirkland, WA, USA*, 2017.

[6] E. Sisinni, A. Depari, A. Flammini, S. Rinaldi, and P. Ferrari, "Evaluating the joint use of lorawan and bluetooth mesh to improve survivability for critical sensor applications," *IEEE Sensors Journal*, 2024.

[7] G. V. Zaruba, S. Basagni, and I. Chlamtac, "Bluetrees-scatternet formation to enable bluetooth-based ad hoc networks," in *ICC 2001. IEEE International Conference on Communications. Conference Record (Cat. No. 01CH37240)*, vol. 1. IEEE, 2001, pp. 273–277.

[8] P. McDermott-Wells, "Bluetooth scatternet models," *IEEE potentials*, vol. 23, no. 5, pp. 36–39, 2004.

[9] M. Baert, J. Rossey, A. Shahid, and J. Hoebeke, "The bluetooth mesh standard: An overview and experimental evaluation," *Sensors*, vol. 18, no. 8, p. 2409, 2018.

[10] R. Rondón, A. Mahmood, S. Grimaldi, and M. Gidlund, "Understanding the performance of bluetooth mesh: Reliability, delay, and scalability analysis," *IEEE Internet of things journal*, vol. 7, no. 3, pp. 2089–2101, 2019.

[11] J. Wieme, M. Baert, and J. Hoebeke, "Managing a qos-enabled bluetooth mesh network using a digital twin network: An experimental evaluation," *Internet of Things*, vol. 25, p. 101023, 2024.

[12] A. Aijaz, "Infrastructure-less wireless connectivity for mobile robotic systems in logistics: Why bluetooth mesh networking is important?" in *2021 26th IEEE International Conference on Emerging Technologies and Factory Automation (ETFA)*. IEEE, 2021, pp. 1–8.

[13] E. De Leon and M. Nabi, "An experimental performance evaluation of bluetooth mesh technology for monitoring applications," in *2020 IEEE Wireless Communications and Networking Conference (WCNC)*. IEEE, 2020, pp. 1–6.

[14] F. Álvarez, L. Almon, H. Radtki, and M. Hollick, "Bluemergency: Mediating post-disaster communication systems using the internet of things and bluetooth mesh," in *2019 IEEE Global Humanitarian Technology Conference (GHTC)*. IEEE, 2019, pp. 1–8.

[15] M. P. JV, B. J. O. de Souza, and M. Endler, "Exploring data collection on bluetooth mesh networks," *Ad Hoc Networks*, vol. 130, p. 102809, 2022.

[16] "Mesh Networking Specifications | Bluetooth® Technology Website," *Bluetooth Mesh*, pp. 1–333, November 2020. [Online]. Available: https://www.bluetooth.com/specifications/mesh-specifications/

[17] J. Tosi, F. Taffoni, M. Santacatterina, R. Sannino, and D. Formica, "Performance evaluation of bluetooth low energy: A systematic review," *Sensors*, vol. 17, no. 12, p. 2898, 2017.

[18] D. Perez-Diaz-de Cerio, Á. Hernández-Solana, M. García-Lozano, A. V. Bardají, and J.-L. Valenzuela, "Speeding up bluetooth mesh," *IEEE Access*, vol. 9, pp. 93 267–93 284, 2021.

[19] "Core Specifications | Bluetooth® Technology Website," *Bluetooth Low Energy*, pp. 1–3256, November 2020. [Online]. Available: https://www.bluetooth.com/specifications/bluetooth-core-specification

[20] J. D. Gotz, O. K. Rayel, and G. L. Moritz, "Improving bluetooth mesh energy efficiency using clustering," *Journal of Communication and Information Systems*, vol. 36, no. 1, pp. 156–165, 2021.

[21] M. Reno, R. Rondón, L. L. Bello, G. Patti, A. Mahmood, A. Lombardo, and M. Gidlund, "Relay node selection in bluetooth mesh networks," in *2020 IEEE 20th Mediterranean Electrotechnical Conference (MELECON)*. IEEE, 2020, pp. 175–180.

[22] E. A. Hansen, M. H. Nielsen, D. E. Serup, R. J. Williams, T. K. Madsen, and R. Abildgren, “On relay selection approaches in bluetooth mesh networks,” in *2018 10th International Congress on Ultra Modern Telecommunications and Control Systems and Workshops (ICUMT)*. IEEE, 2018, pp. 1–5.
[23] D. Hortelano, T. Olivares, and M. C. Ruiz, “Reducing the energy consumption of the friendship mechanism in bluetooth mesh,” *Computer Networks*, vol. 195, p. 108172, 2021.
[24] B. Lin and H. Su, “Experimental evaluation and performance improvement of bluetooth mesh network with broadcast storm,” *IEEE Access*, 2023.
[25] D. Perez-Diaz-de Cerio, J. L. Valenzuela, M. Garcia-Lozano, Á. Hernández-Solana, and A. Valdovinos, “BMADS: BLE mesh asynchronous dynamic scanning,” *IEEE Internet of Things Journal*, vol. 8, no. 4, pp. 2558–2573, 2020.
[26] Z. Hosseinkhani and M. Nabi, “BMSim: an event-driven simulator for performance evaluation of bluetooth mesh networks,” *IEEE Internet of Things Journal*, pp. 1–1, 2023.
[27] “Mobility model.” [Online]. Available: https://github.com/panisson/pymobility
[28] S. M. Darroudi, C. Gomez, and J. Crowcroft, “Bluetooth low energy mesh networks: A standards perspective,” *IEEE Communications Magazine*, vol. 58, no. 4, pp. 95–101, 2020.
[29] P. Pierleoni, A. Gentili, M. Mercuri, A. Belli, R. Garello, and L. Palma, “Performance improvement on reception confirmation messages in bluetooth mesh networks,” *IEEE Internet of Things Journal*, 2021.
[30] T. Camp, J. Boleng, and V. Davies, “A survey of mobility models for ad hoc network research,” *Wireless communications and mobile computing*, vol. 2, no. 5, pp. 483–502, 2002.
[31] H. Barbosa, M. Barthelemy, G. Ghoshal, C. R. James, M. Lenormand, T. Louail, R. Menezes, J. J. Ramasco, F. Simini, and M. Tomasini, “Human mobility: Models and applications,” *Physics Reports*, vol. 734, pp. 1–74, 2018.

Zohreh Hosseinkhani received her B.Sc. and M.Sc. degrees in Computer Engineering from Electrical and Computer Engineering Department of the Isfahan University of Technology, Isfahan, Iran, in 2014 and 2016, respectively. She completed her Ph.D. in Computer Engineering at the same university in 2024. Her research interests include the Internet of Things (IoT), wireless sensor networks, Bluetooth Mesh networks, and machine learning.

Carles Gomez obtained his Ph.D. thesis in Network Engineering in 2007. He is a Full Professor at the Universitat Politecnica de Catalunya (UPC). He is a co-author of numerous papers published in journals and conferences, as well as IETF RFCs and Internet Drafts. He is an IETF 6Lo Working Group Chair. He serves as an editorial board member for several journals. His research interests mainly focus on the Internet of Things and deep space communication.

Majid Nabi (Member, IEEE) received the B.Sc. degree in computer engineering from Isfahan University of Technology, Isfahan, Iran, in 2001, the M.Sc. degree in computer engineering from Tehran University, Tehran, Iran, in 2007, and the Ph.D. degree in electrical and computer engineering from Eindhoven University of Technology (TU/e), Eindhoven, The Netherlands, in 2013.

He is currently an Assistant Professor at the Department of Electrical Engineering, TU/e. His research interests include efficient and reliable networked embedded systems, low-power wireless sensor networks, Internet of Things, and efficient machine learning techniques for network management.